

Accuracy versus time frontiers of semi-supervised and self-supervised learning on medical images

Zhe Huang^{1,*}, Ruijie Jiang^{2,*}, Shuchin Aeron^{1,2}, and Michael C. Hughes¹

¹Dept. of Computer Science, Tufts University

²Dept. of Electrical & Computer Engineering, Tufts University

*Lead authors ZH & RJ contributed equally

Abstract

For many applications of classifiers to medical images, a trustworthy label for each image can be difficult or expensive to obtain. In contrast, images *without* labels are more readily available. Two major research directions both promise that additional unlabeled data can improve classifier performance: self-supervised learning pretrains useful representations on unlabeled data only, then fine-tunes a classifier on these representations via the labeled set; semi-supervised learning directly trains a classifier on labeled and unlabeled data simultaneously. Recent methods from both directions have claimed significant gains on non-medical tasks, but do not systematically assess medical images and mostly compare only to methods in the same direction. This study contributes a carefully-designed benchmark to help answer a practitioner’s key question: given a small labeled dataset and a limited budget of hours to spend on training, what gains from additional unlabeled images are possible and which methods best achieve them? Unlike previous benchmarks, ours uses realistic-sized validation sets to select hyperparameters, assesses runtime-performance tradeoffs, and bridges two research fields. By comparing 6 semi-supervised methods and 5 self-supervised methods to strong labeled-only baselines on 3 medical datasets with 30-1000 labels per class, we offer insights to resource-constrained, results-focused practitioners: MixMatch, SimCLR, and BYOL represent strong choices that were not surpassed by more recent methods. After much effort selecting hyperparameters on one dataset, we publish settings that enable strong methods to perform well on new medical tasks within a few hours, with further search over dozens of hours delivering modest additional gains.

1 INTRODUCTION

Deep neural networks can deliver exceptional performance on classification tasks when trained with vast labeled datasets. However, in medical imaging applications assembling a large dataset where each image is associated with an appropriate label can be prohibitively costly due to manual effort required by a human expert. In contrast, images alone, without labels, are often readily available in health records databases. Over recent years, considerable research effort has been expended to develop methods that can use a large additional unlabeled dataset together with a small labeled set to train image classifiers, striving to outperform methods trained only on the labeled set.

Two ways of leveraging unlabeled data are particularly popular. First, in *semi-supervised* learning (Zhu, 2005; Van Engelen and Hoos, 2020), recent efforts train deep classifiers *jointly* (Sohn et al., 2020; Berthelot et al., 2019) using an objective with two loss terms, one favoring labeled-set accuracy and the other favoring label-consistency or label-smoothness when extrapolating to the unlabeled set. Alternatively, *self-supervised* methods (Qi and Luo, 2020) focus on a two-stage approach, first training deep representations on the larger unlabeled set, then later fine-tuning a classifier on the

Open-source code [MIT license]: <https://github.com/tufts-ml/SSL-vs-SSL-benchmark>

labeled set. Exemplars are numerous (Oord et al., 2018; Chen et al., 2020b; He et al., 2020; Chen et al., 2020d; Caron et al., 2020; Chen and He, 2021). Despite the remarkable progress reported in each direction, these two paradigms – semi- and self-supervised, each often abbreviated as *SSL* – have been primarily developed independently (Chen et al., 2022). A direct comparison of the two paradigms has been notably absent, especially in a medical context.

This study develops an open-source benchmark intended to help practitioners leverage unlabeled data to tackle new medical image classification challenges where only modest-sized labeled datasets exist. We specifically target a setting with roughly 4-10 class labels of interest, where each class has 30-1000 available labeled images for all model development (including training and validation). We identify representative tasks on 3 datasets that span low-resolution (28x28) to moderate-resolution (112x112) settings. We run careful experiments with over a dozen recent methods across 3 datasets to clarify what gains are possible with unlabeled data and which methods best achieve them.

We emphasize realism throughout, in 5 distinct ways: (1) expecting natural *imbalance* between class sizes; (2) performing extensive *hyperparameter search* following a common protocol; (3) enforcing for each method a *maximum runtime budget* of up to 100 hours for all model development (training and hyperparameter search) on the same hardware (one NVIDIA A100 GPU); (4) *profiling performance over time*, to inform labs with smaller runtime budgets, and (5) *exclusively using realistic-sized validation sets*, avoiding the unfortunately common practice in other published benchmarks of validation sets that are far larger than the training set (see Table 1).

The contributions of this study are:

1. A **systematic comparison of semi-supervised and self-supervised methods**, providing a common evaluation to connect two research directions that have been heretofore mostly disconnected.
2. A **realistic experimental protocol** for fairly evaluating such methods, designed to consider the same constraints on available labels and runtime that practitioners face when applying such methods to new datasets. This avoids unrealistic aspects of past benchmarks, especially the use of far too large validation sets and industrial-scale budgets for hyperparameter search.
3. **Actionable insights about which learning methods and hyperparameter selection strategies perform best** in our context. The primary findings from our experiments are
 - (a) Among semi-supervised methods, we recommend MixMatch as a strong default choice. It performs competitively on all 3 datasets across all time budgets, and was not outperformed by more recent methods like FixMatch or FlexMatch.
 - (b) Among self-supervised methods, we recommend SimCLR or BYOL as strong default choices, as they achieve the best performance across all three datasets.
 - (c) Hyperparameter search is important, and still viable on our realistic-sized validation sets. Extensive search over dozens of hours yields improved results on each dataset.
 - (d) If dataset-specific hyperparameter tuning is unaffordable, we show that direct transfer of the best hyperparameter settings from another source dataset can work well for semi-supervised methods, provided the source is similar enough (e.g. another medical task, not CIFAR-10).

Ultimately, we hope this study guides practitioners with limited data and computational resources toward successful use of semi- and self-supervised learning methods on real problems.

2 BACKGROUND AND CHOSEN METHODS

Unified Problem Formulation. Following the recent survey by Chen et al. (2022), we adopt a unified perspective on using supervised learning, semi-supervised learning, self-supervised learning techniques to train image classifiers for real applications with limited available labeled data. For model development (including training and hyperparameter selection), we assume there are two available datasets. First, a labeled dataset \mathcal{L} of many feature-label pairs (x, y) , where each image is represented by a D -dimensional feature vector $x \in \mathbb{R}^D$ and its corresponding class label takes one of C possible values: $y \in \{1, 2, \dots, C\}$. Second, an optional unlabeled set \mathcal{U} of feature vectors. Typically, we assume the unlabeled set is much larger: $|\mathcal{U}| \gg |\mathcal{L}|$.

Given labeled set \mathcal{L} and unlabeled set \mathcal{U} , we wish to train a neural network that can map each x to probability vector in the C -dimensional simplex Δ^C representing a distribution over C class labels. Let $f_v(\cdot) : \mathbb{R}^D \rightarrow \mathbb{R}^F$ denote a representation layer producing F -dimensional embedding given any input image with neural parameters v , and $g_w(\cdot) : \mathbb{R}^F \rightarrow \Delta^C$ denote a final softmax classification

Benchmark	Val. set size	Acc.-runtime tradeoff?	Methods.
Realistic eval. of SSL (Oliver et al., 2018)	unrealistic	NO	Semi. only
SSL for fine-grained clf. (Su et al., 2021)	unrealistic	NO	Semi & 1 Self*
USB (Wang et al., 2022)	unrealistic	NO	Semi. only
Self benchmark (Ericsson et al., 2021)	no val. set	NO	Self only
SSL-vs-SSL (ours)	realistic	YES	6 Semi & 5 Self

Table 1: Comparison of related work on benchmarking semi-supervised learning and self-supervised learning. *: Su et al. focus on semi-supervised, but do include one self-supervised method (MOCO) in their benchmark.

layer with linear weights w . The following unified objective can capture all three learning paradigms:

$$v^*, w^* \leftarrow \arg \min_{v, w} \sum_{x, y \in \mathcal{L}} \lambda^L \ell^L(y, g_w(f_v(x))) + \sum_{x \in \mathcal{U}} \lambda^U \ell^U(x, f_v, g_w) \quad (1)$$

where ℓ^L represents a labeled-set loss (e.g. multi-class cross-entropy), while ℓ^U represents a unlabeled-set loss and $\lambda^L, \lambda^U > 0$ are weights for the corresponding loss terms. The design of ℓ^U is usually what differs substantially across the semi- and self-supervised methods. Setting ℓ^U to be cross-entropy computed with pseudo-labels generated from classifier g recovers PseudoLabel (Lee, 2013); a temperature-scaled instance-similarity contrastive loss to recovers SimCLR (Chen et al., 2020b).

All three learning paradigms we study optimize Eq. (1), differing in the number of phases and in how to set the scalar weights λ^L, λ^U on each loss term. Supervised learning sets the unlabeled weight $\lambda^U = 0$ throughout, thus learning all weights using only the labeled set. Semi-supervised methods include both terms in one end-to-end training, using $\lambda^U > 0$ and $\lambda^L > 0$. Self-supervised learning has two phases. In phase 1 (“pretraining”), the labeled term is omitted ($\lambda^L = 0, \lambda^U = 1$) and the focus of learning is an effective representation layer f_v (classifier g_w is not included in this phase). In phase 2 (“fine-tuning”), we focus on the labeled term and the unlabeled term is omitted ($\lambda^L = 1, \lambda^U = 0$). We fix the learned representation layer parameter v and fine-tune the classifier w .

Supervised methods. The goal of leveraging unlabeled data \mathcal{U} is to obtain better performance than what we could obtain using only the labeled set \mathcal{L} . Therefore, a natural baseline for our study is any model that trains only on the labeled data \mathcal{L} . We pursue 3 high-quality baselines of this type. First, a standard “labeled-only” baseline that trains using only the labeled set with loss ℓ^L set to multi-class cross-entropy. Second, “mixup” trains with cross entropy with the addition of mixup data augmentation (Zhang et al., 2017). Finally, “Sup. Contrast” pursues a supervised contrastive learning loss for ℓ^L (Khosla et al., 2020). These baselines (esp. the latter two) represent modern ways to squeeze the most out of a limited labeled set *without* any extra unlabeled data.

Semi-supervised methods. For this study, we implement 6 semi-supervised methods that can train deep classifiers on both labeled and unlabeled data *simultaneously*, as in Eq. (1). As representative of the state-of-the-art in semi-supervised learning for image classification tasks, our selected methods are: Pseudo Labeling (Lee, 2013), Mean Teacher (Tarvainen and Valpola, 2017), MixMatch (Berthelot et al., 2019), FixMatch (Sohn et al., 2020) and FlexMatch (Zhang et al., 2021). CoMatch (Li et al., 2021) is a 6th method that represents a combination of self-supervised and semi-supervised methodology. These choices cover a reasonably wide spectrum of year of publication, design of unlabeled loss, and computation cost. See Appendix for a wider literature review.

Self-supervised methods. For our study, we implement 5 self-supervised learning algorithms: SimCLR (Chen et al., 2020b), MOCO (v2) (He et al., 2020; Chen et al., 2020d), SwAV (Caron et al., 2020), BYOL (Grill et al., 2020) and SimSiam (Chen and He, 2021). The above five algorithms epitomize the field of self-supervised learning as of this writing. SimCLR, MOCO (v2), and SwAV are all based on contrastive learning, which requires both similar and dissimilar samples. In contrast, BYOL was designed to circumvent the need for dissimilar samples. Lastly, SimSiam was introduced as the most simplified framework for self-supervised learning.

3 RELATED WORK

Table 1 compares the key attributes of existing major benchmarks for semi-supervised and self-supervised methods and situates our present study in this context.

Prior semi-supervised benchmarks. Oliver et al. (2018) benchmarked deep semi-supervised learning algorithms from several unique angles, including varying the amount of labeled and unlabeled data and comparing to transfer learning. Their experiments provided useful insights to the semi-supervised learning community. Oliver et al. further pointed out the common issue of unrealistically

large validation sets in typical experimental settings. However, their experiments *still use* this unrealistic setting. Instead, **we benchmark algorithms using realistically-sized train/validation splits**, mimicking what practitioners would face in real-applications. Furthermore, while [Oliver et al.](#) stressed the importance of fair hyperparameter search, their reported results were based on “*1000 trials of Gaussian Process-based black box optimization using Google Cloud ML engine*”. This is impractical for researchers who are not affiliated with highly-resourced industrial labs. Their focus on final performance also masks the dynamics of the performance versus computation tradeoff, which renders it less insightful for practitioners with new dataset at hand with limited resource available trying to seek the best outcome under these constraints. To address this, **we give each algorithm a fixed computation budget of some hours, and analyse how performance progresses over time.** TorchSSL ([Zhang et al., 2021](#)) benchmarked eight popular semi-supervised learning algorithm using a unified codebase. The same group later extended prior benchmarking efforts that mainly focus on image domain to natural language processing and audio processing via a new benchmark called USB ([Wang et al., 2022](#)). They further use pre-trained Transformer ([Vaswani et al., 2017](#); [Dosovitskiy et al., 2020](#)) on ImageNet-1K ([Russakovsky et al., 2015](#)) and found that pretraining could be beneficial to semi-supervised learning. However, for new medical imaging datasets, it is non-trivial to find a similar-enough dataset for such a pre-training. Finally, a recent SSL benchmark for fine-grained classification by [Su et al. \(2021\)](#) evaluates semi-supervised learning on datasets that exhibit class imbalance and contains images from novel classes in the unlabeled set, studying the effect of different initializations and the contents of unlabeled data on the performance of semi-supervised methods.

Prior self-supervised benchmarks. Several works have proposed different benchmarks for self-supervised methods on various tasks and domains. [Goyal et al. \(2019\)](#) introduced a benchmark that covers 9 different datasets and tasks, such as object detection, surface normal estimation, and visual navigation. [Ericsson et al. \(2021\)](#) compared thirteen top self-supervised models on 40 downstream tasks. [Da Costa et al. \(2022\)](#) presented a library of self-supervised methods that can be easily plugged into different downstream tasks and datasets. However, a few aspects of these benchmarks do not cover the realistic needs of practitioners in our setting. First, they do not incorporate the use of a validation set (which can lead to suboptimal accuracy at test time and complicate comparisons to methods that do tune on validation sets). Second, they do not consider accuracy changes over time.

Combining Semi- and Self-supervision. An active line of research has explored the *fusion* of semi-supervised learning and self-supervised learning ideas ([Zhai et al., 2019](#); [Kim et al., 2021](#); [Li et al., 2021](#); [Zheng et al., 2022](#)). Some recent surveys ([Qi and Luo, 2020](#); [Chen et al., 2022](#)) comprehensively compare semi-supervised and self-supervised learning methods, but they focus on literature review while we offer realistic and comprehensive benchmarking experiments.

4 DATASETS AND TASKS

We utilize three medical image classification datasets in this study, all with 2D images. Two are lightweight datasets whose low resolution (28x28) is ideal for rapid prototyping of new algorithms. We selected PathMNIST and TissueMNIST from 12 candidate datasets in the MedMNIST collections ([Yang et al., 2021, 2023](#)) by matching two criteria: (i) contains at least 5 imbalanced classes, and (ii) can build a large unlabeled set (at least 50000 images). The last dataset is the Tufts Medical Echocardiogram Dataset (TMED-2), a dataset with higher resolution (112x112) specifically collected to represent an authentic assessment of methods for limited labeled data. Dataset statistics, especially train/validation/test split counts by class, are provided in Table 2.

For each dataset, we pursue a data splitting strategy that closely mirrors the conditions a practitioner would encounter in trying to apply SSL methods to a smaller labeled set and a much larger unlabeled set. First, we make sure training and validation sets contain a natural distribution of classes even if that may be imbalanced. This reflects how data would likely be affordably collected (by random sampling) and avoids artificially balanced training sets that will not match the population an algorithm is expected to encounter in a deployment. Second, we force training set and validation set sizes to be realistic. This is in contrast to previous benchmarks like USB ([Wang et al., 2022](#)), which used TissueMNIST but did all hyperparameter search on large validation set of 23,640 images even though the labeled training set contained only 80 or 400 images. In practice, such a large validation set would almost certainly be split differently to improve training, as noted in [Oliver et al. \(2018\)](#).

TissueMNIST is a lightweight dataset of 28x28 images of human kidney cortex cells, segmented from 3 reference tissue specimens and organized into 8 categories. The original dataset is fully-labeled and distributed with predefined train/val/test split of 165,466/23,640/47,280 images with

(a) TissueMNIST					(b) PathMNIST					(c) TMED-2				
28x28 kidney cell images					28x28 colorectal cancer slides					112x112 ultrasound of heart				
		Labeled		Unlabeled			Labeled		Unlabeled			Labeled		Unlabeled
		Train	Val	Test			Train	Val	Test			Train	Val	Test
total	400	400	47280	165066	total	450	450	7180	89546	total	1660	235	2019	353,500
class2	15	15	1677	5851	class6	39	39	741	7847	class1	223	50	342	-
class1	19	19	2233	7795	class4	40	40	1035	7966	class3	325	28	319	-
class5	19	19	2202	7686	class0	47	47	1338	9319	class2	462	39	423	-
class4	28	28	3369	11761	class7	47	47	421	9354	class0	650	118	935	-
class3	37	37	4402	15369	class1	48	48	847	9461					
class7	59	59	7031	24549	class2	52	52	339	10308					
class6	95	95	11201	39108	class3	52	52	643	10349					
class0	128	128	15165	52947	class5	61	61	592	12121					
					class8	64	64	1233	12821					

Table 2: **Summary statistics of train/validation/test splits** for all 3 datasets in our study. Each table’s rows are arranged in ascending order based on the number of per-class labeled train images.

some class imbalance. We assume a total labeling budget of 800 images, evenly split between training and validation so that validation-based hyperparameter tuning may be reliable. We form a labeled training set of 400 images from the predefined training set, sampling each class by its frequency in original training set (in many medical applications, this frequency can often be determined using prior knowledge). Similarly, we form a labeled validation set of 400 images from the predefined validation set. Our resulting data splits are in Table 2. All experiments report performance on the complete predefined test set. For unlabeled data, we keep all remaining images in the original training split, discarding known labels.

PathMNIST is another lightweight dataset of 28x28 images of patches from colorectal cancer histology slides. The dataset is comprised of 9 types of tissues, resulting in a 9-class multi-class classification task. The creators’ predefined train/val/test split is of 89,996/10,004/7,180 images. There is class imbalance, but less severe than TissueMNIST. We assume a total labeling budget of 900 images, again evenly split between training and validation. We form a labeled training set of 450 images from the predefined training set, sampling each class by its original train set frequency.

TMED-2 (Huang et al., 2021, 2022) is an open-access dataset of 112x112 2D grayscale images captured from routine echocardiogram scans. Each scan produces dozens of ultrasound images of the heart, captured from multiple acquisition angles (i.e., different anatomic views). In this study, we adopt Huang et al.’s view-classification task: the goal is to classify whether an image corresponds to parasternal long axis (PLAX), parasternal short axis (PSAX), apical 2-chamber (A2C) or apical 4-chamber (A4C) view. View classification is clinically important: meaningful downstream measurements or diagnoses of heart disease can only be made when looking at the right anatomical view (Madani et al., 2018; Wessler et al., 2023). We used the provided predefined train/validation/test split (id #1), which is reasonably sized and imbalanced by design. We further use the provided large unlabeled set of 353,500 images. We emphasize that this unlabeled set is both *authentic* (no true labels are available at all, unlike other benchmarks that “forget” known labels) and *uncurated* (Huang et al., 2023) (contains images of view types beyond the 4 classes of interest in the labeled task).

5 EXPERIMENTAL DESIGN

Performance metric. We use *balanced accuracy* (Guyon et al., 2015; Grandini et al., 2020) as our primary performance metric. For a task with $C > 2$ classes, let $y_{1:N}$ denote true labels for N examples in a test set, and $\hat{y}_{1:N}$ denote a classifier’s predicted labels. Let $\text{TP}_c(\cdot)$ count *true positives* for class c (number of correctly classified examples whose true label is c), and let $N_c(\cdot)$ count the total number of examples with true label c . Then we compute balanced accuracy as a percentage:

$$\text{balanced-accuracy}(y_{1:N}, \hat{y}_{1:N}) = \frac{1}{C} \sum_{c=1}^C \frac{\text{TP}_c(y_{1:N}, \hat{y}_{1:N})}{N_c(y_{1:N})} \cdot 100\%. \quad (2)$$

Balanced accuracy is more suitable than standard accuracy for assessing imbalanced problems when each class matters equally. The expected balanced accuracy of a uniform random guess is $\frac{100}{C}\%$.

Architectures. To fairly compare methods, we use the same backbone f_v : ResNet-18 (He et al., 2016) on Tissue and Path, and Wide ResNet-28-2 (Zagoruyko and Komodakis, 2016) on TMED-2.

Training with early stopping. For each training phase, we perform gradient descent learning on Eq. (1) with Adam (Kingma and Ba, 2014) that traverses minibatches of labeled and unlabeled sets, using a cosine learning rate schedule. Each training phase proceeds for up to 200 epochs, where one epoch represents enough minibatch updates to process the equivalent of the entire dataset $\mathcal{L} \cup \mathcal{U}$. After every epoch, we record balanced accuracy on the validation set. If this value plateaus for 20 consecutive epochs, we stop the current training phase early.

Hyperparameters. Semi- and self-supervised learning can both be sensitive to hyperparameters (Su et al., 2021; Wagner et al., 2022). Hyperparameters that need to be tuned include some common to many algorithms (e.g. learning rates, weight decay, unlabeled loss weight λ^U) and those unique to each algorithm. See App. C.1 for reproducible details on all hyperparameters for our 14 methods.

Unified algorithm for training and hyperparameter search. We formulate a unified procedure mindful of realistic hardware and runtime constraints for a non-industrial-scale lab working on a new medical dataset. We assume each of the 14 algorithms assessed (including supervised, semi-supervised, and self-supervised methods) has access to one NVIDIA A100 GPU for a fixed number of hours. Within the allotted time budget, for each method we execute a serial random search over hyperparameters, sequentially sampling each new configuration and then training until the early stopping or maximum epoch is reached. Every 30 minutes (and every epoch), we track the best-so-far classifier in terms of validation-set balanced accuracy. Algorithm B.1 provides pseudocode. Each time a new hyperparameter configuration is needed, we sample each hyperparameter value independently from a distribution designed to cover its common settings in prior literature. Our choice of random search on a budget is thought to yield better performance than grid search (Bergstra and Bengio, 2012), fairly expends the same effort to train all methods regardless of their cost-per-epoch or hyperparameter complexity, and does not assume industrial-scale access to 1000 cloud-computing trials as in Oliver et al. (2018). As a rule of thumb, we find that performance saturates after about 25 hours per 80000 unlabeled examples. We thus allocate for the total time budget 25 hours for PathMNIST, 50 hours for TissueMNIST, and 100 hours for TMED-2.

Data augmentation. Following common practice, random flip and crop augmentations are used for all semi-supervised learning algorithms as well as “labeled-only” and “MixUp”. MixMatch further utilizes MixUp (Zhang et al., 2017), while RandAugment (Cubuk et al., 2020) is used in FixMatch and FlexMatch. For each self-supervised method as well as “Sup Contrast” baseline, we apply the same SimCLR augmentation: random flip, crop, color jitter, and grayscale.

Multiple trials. We repeat Alg. B.1 for each method across 5 separate trials (distinct random seeds). We record the mean balanced accuracy across these trials on the test set at each 30 minute interval. When helpful, we also report variability across trials via the (min, max) interval of these 5 trials.

6 RESULTS & ANALYSIS

Comparing semi- and self- methods. Fig. 1 plots each method’s progress in balanced accuracy (averaged across 5 trials) as a function of model development time. We emphasize the best checkpoint at each 30 minute interval is selected on validation set, and then we report that checkpoint’s test-set balanced accuracy. Similar plots in App. A show the profiles using initial weights pretrained on ImageNet, rather than random initial weights. From these figures, the major findings are:

- **Using realistically-sized validation sets for hyperparameter search and checkpoint selection can be effective.** All 14 methods show roughly monotonic improvements in test accuracy over time, despite using a realistic-sized validation set. Cautions from Oliver et al. (2018) about high variance estimates from such small sets are warranted, but we think this empirical success is enough to suggest future work avoid the unrealistically large validation sets of past benchmarks.
- **MixMatch is recommended among all semi-supervised methods.** MixMatch (and other new semi-supervised methods) consistently perform better than any pre-2019 methods, while MixMatch itself is not really ever surpassed by newer methods FixMatch, FlexMatch, or CoMatch.
- **SimCLR and BYOL are the recommended self-supervised methods.** The performance of SimCLR and BYOL improves the fastest. Additionally, under the same running time, SimCLR and BYOL consistently achieve the best performance compared to the other three methods.
- The rankings of top-performing methods do not change much if we use initial weights fit to ImageNet, rather than initializing randomly (see Fig. A.1). We also do not see notable gains in ultimate test-set accuracy when top methods use pretraining. With this in mind, pretraining does still seem to be beneficial (improves convergence speed and reliability across trials).

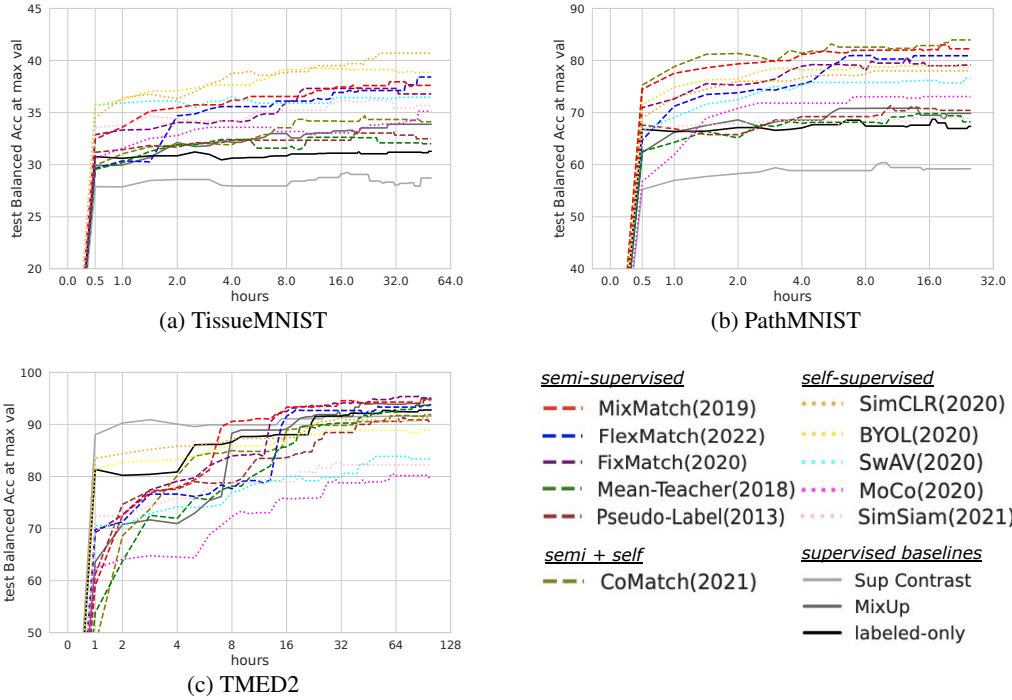


Figure 1: **Test accuracy over time profiles of semi- and self-supervised methods on 3 datasets (panels a-c).** At each time, we report mean of each method over 5 trials of Alg. B.1. On TissueMNIST (a), SimCLR (orange) and BYOL (yellow) are dominant from 1 hour onward. On PathMNIST (b), MixMatch (red) and CoMatch (olive) are dominant from 1 hour onward, On TMED-2 (c), Sup Contrast wins for first 7 hours, then MixMatch overtakes it, eventually joined (not surpassed) by FixMatch and FlexMatch.

Reliability across trials. Fig. 2 (left) shows the range (low-high) across 5 trials in balanced accuracy on both validation and test sets for each algorithm on select datasets and time horizons (complete plots for all datasets are in App. A.) Unsurprisingly, after only a few hours we see high variation for all methods, especially for semi-supervised methods. As time goes on, there is a notable reduction in variation. This suggests that sufficient compute budget is needed for our hyperparameter search.

Consistency in validation vs. test scores. Tab. 3 (right) reports an average for all “semi-”supervised and all “self-”supervised methods of the discrepancy in balanced accuracy between the maximum validation score and the corresponding test score. On all 3 datasets, the generalization gap for self-supervised is closer to zero. This suggests self-supervised learning may offer more consistent estimates of generalization potential under the conditions of our experiments; semi-supervised validation performance is usually too optimistic.

Cost-benefit comparison of hyperparameter transfer strategies.

To make the most of limited labeled data, one potential strategy is to use the entire labeled set for training, reserving no validation set at all. This approach relies on pre-established hyperparameters, sourced from other datasets, obviating the need for hyperparameter tuning. Su et al. (2021) employed this strategy in their benchmarking effort, suggesting tuning on small-validation sets would likely yield unreliable or suboptimal accuracy without direct experimental comparison.

Here, we compare these two strategies: our suggested hyperparameter search (Alg. B.1) on a realistically-sized validation set versus utilizing all labeled data for training with off-the-shelf hyperparameters derived from another dataset (“from TissueMNIST” or “from CIFAR-10”). We train the latter for 100 epochs on PathMNIST and 80 epochs on TMED2. Training is terminated early if the train loss does not improve over 20 consecutive epochs (full details in App. B.2). Empirically, we observe that all models which did not trigger early stopping reached a plateau in training loss.

	Acc(val) - Acc(test)		
	Tissue	Path	TMED
Semi	8.25	11.22	4.33
Self	6.88	-0.06	3.86

Table 3: **Generalization gap on each dataset** (closer-to-zero indicates more reliability), after the maximum allotted time. Self-supervised methods in aggregate appear to have a lower validation-test gap (less risk of overfitting).

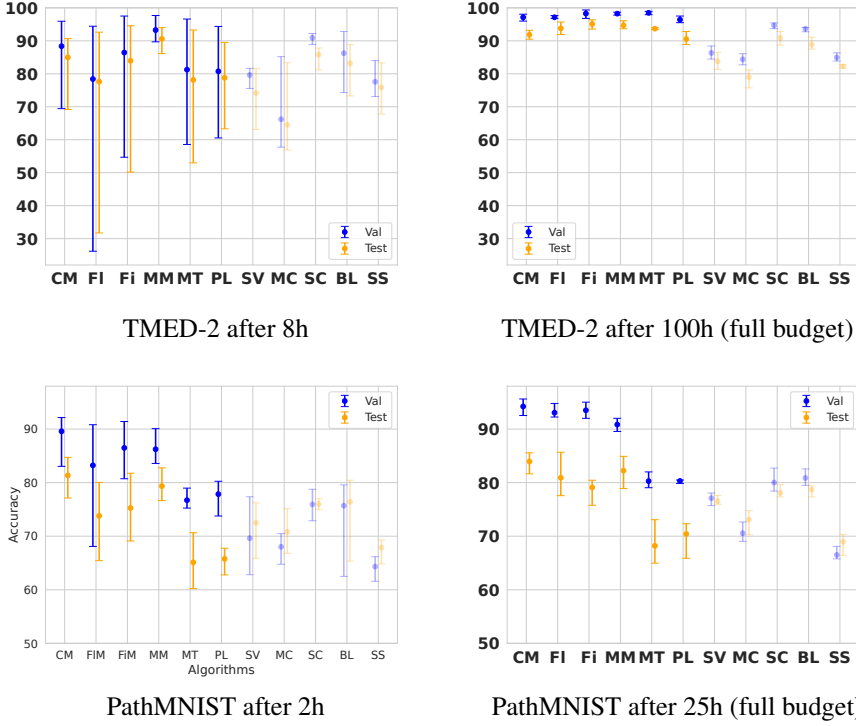


Figure 2: **Performance variation across independent trials over time.** Intervals visualize the lowest and highest balanced accuracy of 5 separate trials of Alg. B.1. Y-axis shows balanced accuracy. X-axis from left to right shows CoMatch, FlexMatch, FixMatch, MixMatch, Mean-Teacher, Pseudo-labeling, SwAV, MoCo, SimCLR, BYOL and SimSiam. More results in Appendix A.

Tab. 4 shows the final test-set balanced accuracy achieved by each strategy on the PathMNIST and TMED-2 datasets. From this table, the major findings are:

- Complete hyperparameter search on the target dataset is competitive (see all the green cells under “Hyper search.” column of Tab. 4). However, it does require the greatest runtime (25+ hr).
- Transfer of best hyperparameters from another medical dataset (“from Tissue”) seems to be viable, especially for strong semi-supervised methods like MixMatch, FixMatch, or FlexMatch. On PathMNIST, this strategy is much faster (< 4 hr) than the full search.
- Transfer of best hyperparameters from less similar datasets, such as the non-medical CIFAR-10, is less preferred (see all red cells in Tab. 4).
- Using the Su et al. strategy of using all data for training (reserving no validation set) makes selecting an optimal checkpoint challenging. For instance, adjacent epochs that exhibit similar low training losses may have test accuracy varying by over 5%. Thus, we recommend resource-enabled researchers to adopt a realistic validation set strategy.

7 DISCUSSION & CONCLUSION

We have contributed a benchmark that helps practioners quantify what gains in a classification task are possible from the addition of unlabeled data and which methods help achieve them. We offer a unified approach to training and hyperparameter selection of semi-supervised methods, self-supervised methods, and supervised baselines that is both affordable and realistic for research labs tackling new challenges without industrial-scale resources. When using our recommended semi-supervised method (MixMatch), we find that using hyperparameter settings that were tuned over many hours from one source dataset (Tissue) are often “good enough”, delivering high-quality performance on two other target datasets (Path, TMED-2) while making all labeled data available for training. Additional hyperparmater search over dozens of extra hours yielded only modest gains on TMED-2 (up to to 2 points of balanced accuracy). Nevertheless for any new dataset we do recommend trying custom hyperparameter search if possible, as it did yield gains for several methods beyond MixMatch.

PathMNIST					TMED-2				
	Hyper.	from	from	Tissue	Hyper.	from	from	Tissue	
	search	Tissue	CIFAR-10	Time	search	Tissue	CIFAR-10	Time	
semi MixMatch	82.24	83.87	73.51	2.5h	94.71	92.67	74.73	26.1h	
CoMatch	83.95	80.51	86.42	3.4h	91.87	92.51	92.67	47.1h	
FixMatch	79.11	82.64	79.73	2.3h	95.06	95.12	95.73	32.1h	
FlexMatch	80.91	78.70	80.23	2.5h	93.77	93.97	93.70	30.7h	
Pseudo-Label	70.42	66.12	64.71	0.4h	90.52	88.78	82.13	14.1h	
Mean-Teacher	68.21	55.90	56.13	0.5h	93.70	91.21	58.26	18.5h	
self SimCLR	77.63	77.08	76.17	1.6h	92.83	83.08	82.41	8.0h	
BYOL	78.88	79.12	79.88	3.0h	90.52	70.19	71.55	16.2h	
SwAV	76.77	75.51	76.88	2.4h	83.41	73.72	84.10	6.7h	
MoCo	73.63	71.04	73.19	1.0h	81.77	64.20	68.68	11.1h	
SimSiam	68.9	50.84	52.19	0.9h	82.25	45.87	40.46	3.5h	

Table 4: **Hyperparameter strategy evaluation.** Table reports ultimate test-set balanced accuracy on two target datasets: PathMNIST (left) or TMED-2 (right). “Hyper search”: custom hyperparameter search on target via Alg. B.1 for 25 hours (100 for TMED-2). “from Tissue/from CIFAR-10”: just one training phase on the target dataset using the “best” hyperparameters selected from the named source data. We bold best strategy within each row, and color cells relative to this bold value as green (within 2.5 of best), yellow (within 5 of best), and red (worse by 5 or more points). “Tissue Time” reports compute time required for each “from Tissue” result.

Limitations. Our extensive experiments are limited to the 3 datasets we selected. Use caution when extrapolating beyond the dataset sizes, resolutions and class compositions studied here. We deliberately focused on a modest number of labeled examples (30 - 1000) per class, motivated by projects where substantive effort has already gone into labeled data collection. Applications that need to handle more scarce-label regimes (e.g. zero-shot or few-shot methods) may need to look to other benchmarks, as should those looking to classify images into many dozens of classes, especially those with long-tail behavior. We hope our code release enables the medical research community to convert decades of effort on SSL into improved patient outcomes and better scientific understanding of disease and possible treatments. Even for the datasets we study, our analysis here is limited to understanding the performance-time tradeoffs of balanced accuracy. Other clinically useful metrics, such as sensitivity-specificity tradeoffs, calibration, or net benefit, are needed to decide if a classifier is appropriate for deployment (Steyerberg and Vergouwe, 2014). For medical applications, it is also key to understand fairness of methods on various subpopulations (Celi et al., 2022) to avoid propagating structural disadvantages.

Broader impacts. All data analyzed here represent fully-deidentified open-access images, already approved for widespread use by their creators. We think the benefit of promoting these medical tasks to advance ML research outweighs the slight risk of patient reidentification by a future bad actor.

Outlook. Our experiments show that real benefits from the addition of unlabeled data are possible: our recommended methods see gains of +5 points of balanced accuracy on TissueMNIST, +10 points on PathMNIST, and +3 points on TMED-2 against strong labeled-set-only baselines such as Sup Contrast. We hope our code release enables the medical research community to convert decades of effort on SSL into improved patient outcomes and better scientific understanding of disease and possible treatments. We further hope that our benchmark inspires those that pursue improved methodological contributions to favor realistic evaluation protocols.

References

- J. Bergstra and Y. Bengio. Random search for hyper-parameter optimization. *Journal of machine learning research*, 13(2), 2012.
- D. Berthelot, N. Carlini, I. Goodfellow, N. Papernot, A. Oliver, and C. A. Raffel. Mixmatch: A holistic approach to semi-supervised learning. *Advances in neural information processing systems*, 32, 2019.
- A. Blum and T. Mitchell. Combining labeled and unlabeled data with co-training. In *Proceedings of the eleventh annual conference on Computational learning theory*, pages 92–100, 1998.
- T. Brown, B. Mann, N. Ryder, M. Subbiah, J. D. Kaplan, P. Dhariwal, A. Neelakantan, P. Shyam, G. Sastry, A. Askell, et al. Language models are few-shot learners. *Advances in neural information processing systems*, 33:1877–1901, 2020.
- M. Caron, P. Bojanowski, A. Joulin, and M. Douze. Deep clustering for unsupervised learning of visual features. In *Proceedings of the European conference on computer vision (ECCV)*, pages 132–149, 2018.
- M. Caron, I. Misra, J. Mairal, P. Goyal, P. Bojanowski, and A. Joulin. Unsupervised learning of visual features by contrasting cluster assignments. *Advances in neural information processing systems*, 33:9912–9924, 2020.
- P. Cascante-Bonilla, F. Tan, Y. Qi, and V. Ordonez. Curriculum labeling: Revisiting pseudo-labeling for semi-supervised learning. In *Proceedings of the AAAI Conference on Artificial Intelligence*, 2021.
- L. A. Celi, J. Cellini, M.-L. Charpignon, E. C. Dee, F. Dernoncourt, R. Eber, W. G. Mitchell, L. Moukheiber, J. Schirmer, et al. Sources of bias in artificial intelligence that perpetuate healthcare disparities—A global review. *PLOS Digital Health*, 1(3), 2022.
- O. Chapelle, B. Scholkopf, and A. Zien. Semi-supervised learning (chapelle, o. et al., eds.; 2006)[book reviews]. *IEEE Transactions on Neural Networks*, 20(3):542–542, 2009.
- M. Chen, A. Radford, R. Child, J. Wu, H. Jun, D. Luan, and I. Sutskever. Generative pretraining from pixels. In *International conference on machine learning*, pages 1691–1703. PMLR, 2020a.
- T. Chen, S. Kornblith, M. Norouzi, and G. Hinton. A simple framework for contrastive learning of visual representations. In *International conference on machine learning*, pages 1597–1607. PMLR, 2020b.
- T. Chen, S. Kornblith, K. Swersky, M. Norouzi, and G. E. Hinton. Big self-supervised models are strong semi-supervised learners. *Advances in neural information processing systems*, 33: 22243–22255, 2020c.
- X. Chen and K. He. Exploring simple siamese representation learning. In *Proceedings of the IEEE/CVF conference on computer vision and pattern recognition*, pages 15750–15758, 2021.
- X. Chen, H. Fan, R. Girshick, and K. He. Improved baselines with momentum contrastive learning. *arXiv preprint arXiv:2003.04297*, 2020d.
- Y. Chen, M. Mancini, X. Zhu, and Z. Akata. Semi-supervised and unsupervised deep visual learning: A survey. *IEEE Transactions on Pattern Analysis and Machine Intelligence*, 2022.
- E. D. Cubuk, B. Zoph, J. Shlens, and Q. V. Le. Randaugment: Practical automated data augmentation with a reduced search space. In *Proceedings of the IEEE/CVF conference on computer vision and pattern recognition workshops*, pages 702–703, 2020.
- V. G. T. Da Costa, E. Fini, M. Nabi, N. Sebe, and E. Ricci. solo-learn: A library of self-supervised methods for visual representation learning. *J. Mach. Learn. Res.*, 23(56):1–6, 2022.
- J. Devlin, M.-W. Chang, K. Lee, and K. Toutanova. Bert: Pre-training of deep bidirectional transformers for language understanding. *arXiv preprint arXiv:1810.04805*, 2018.

- A. Dosovitskiy, L. Beyer, A. Kolesnikov, D. Weissenborn, X. Zhai, T. Unterthiner, M. Dehghani, M. Minderer, G. Heigold, S. Gelly, et al. An image is worth 16x16 words: Transformers for image recognition at scale. *arXiv preprint arXiv:2010.11929*, 2020.
- L. Ericsson, H. Gouk, and T. M. Hospedales. How well do self-supervised models transfer? In *Proceedings of the IEEE/CVF Conference on Computer Vision and Pattern Recognition*, pages 5414–5423, 2021.
- P. Goyal, D. Mahajan, A. Gupta, and I. Misra. Scaling and benchmarking self-supervised visual representation learning. In *Proceedings of the IEEE/CVF International Conference on computer vision*, pages 6391–6400, 2019.
- M. Grandini, E. Bagli, and G. Visani. Metrics for multi-class classification: an overview. *arXiv preprint arXiv:2008.05756*, 2020.
- J.-B. Grill, F. Strub, F. Altché, C. Tallec, P. Richemond, E. Buchatskaya, C. Doersch, B. Avila Pires, Z. Guo, M. Gheshlaghi Azar, et al. Bootstrap your own latent-a new approach to self-supervised learning. *Advances in neural information processing systems*, 33:21271–21284, 2020.
- I. Guyon, K. Bennett, G. Cawley, H. J. Escalante, S. Escalera, T. K. Ho, N. Macià, B. Ray, M. Saeed, A. Statnikov, et al. Design of the 2015 ChaLearn AutoML challenge. In *2015 International Joint Conference on Neural Networks (IJCNN)*, pages 1–8. IEEE, 2015.
- K. He, X. Zhang, S. Ren, and J. Sun. Deep residual learning for image recognition. In *Proceedings of the IEEE conference on computer vision and pattern recognition*, pages 770–778, 2016.
- K. He, H. Fan, Y. Wu, S. Xie, and R. Girshick. Momentum contrast for unsupervised visual representation learning. In *Proceedings of the IEEE/CVF conference on computer vision and pattern recognition*, pages 9729–9738, 2020.
- Z. Huang, G. Long, B. Wessler, and M. C. Hughes. A new semi-supervised learning benchmark for classifying view and diagnosing aortic stenosis from echocardiograms. In *Proceedings of the Machine Learning for Healthcare Conference*. PMLR, 2021.
- Z. Huang, G. Long, B. S. Wessler, and M. C. Hughes. TMED 2: A dataset for semi-supervised classification of echocardiograms. In *DataPerf: Benchmarking Data for Data-Centric AI Workshop*, 2022.
- Z. Huang, M.-J. Sidhom, B. S. Wessler, and M. C. Hughes. Fix-a-step: Semi-supervised learning from uncurated unlabeled data. In *Proceedings of The 26th International Conference on Artificial Intelligence and Statistics (AISTATS)*, 2023.
- A. Iscen, G. Tolias, Y. Avrithis, and O. Chum. Label propagation for deep semi-supervised learning. In *Proceedings of the IEEE/CVF conference on computer vision and pattern recognition*, pages 5070–5079, 2019.
- L. Jing and Y. Tian. Self-supervised visual feature learning with deep neural networks: A survey. *IEEE transactions on pattern analysis and machine intelligence*, 43(11):4037–4058, 2020.
- P. Khosla, P. Teterwak, C. Wang, A. Sarna, Y. Tian, P. Isola, A. Maschinot, C. Liu, and D. Krishnan. Supervised contrastive learning. *Advances in neural information processing systems*, 33:18661–18673, 2020.
- B. Kim, J. Choo, Y.-D. Kwon, S. Joe, S. Min, and Y. Gwon. Selfmatch: Combining contrastive self-supervision and consistency for semi-supervised learning. *arXiv preprint arXiv:2101.06480*, 2021.
- D. P. Kingma and J. Ba. Adam: A method for stochastic optimization. *arXiv preprint arXiv:1412.6980*, 2014.
- D. P. Kingma, S. Mohamed, D. Jimenez Rezende, and M. Welling. Semi-supervised learning with deep generative models. *Advances in neural information processing systems*, 27, 2014.
- A. Kumar, P. Sattigeri, and T. Fletcher. Semi-supervised learning with gans: Manifold invariance with improved inference. *Advances in neural information processing systems*, 30, 2017.

- S. Laine and T. Aila. Temporal ensembling for semi-supervised learning. *arXiv preprint arXiv:1610.02242*, 2016.
- D.-H. Lee. Pseudo-label: The simple and efficient semi-supervised learning method for deep neural networks. In *Workshop on challenges in representation learning at ICML*, 2013.
- J. Li, C. Xiong, and S. C. Hoi. Comatch: Semi-supervised learning with contrastive graph regularization. In *Proceedings of the IEEE/CVF international conference on computer vision*, pages 9475–9484, 2021.
- A. Madani, R. Arnaout, M. Mofrad, and R. Arnaout. Fast and accurate view classification of echocardiograms using deep learning. *NPJ digital medicine*, 1(1):6, 2018.
- S. Min, X. Chen, H. Xie, Z.-J. Zha, and Y. Zhang. A mutually attentive co-training framework for semi-supervised recognition. *IEEE Transactions on Multimedia*, 23:899–910, 2020.
- A. Oliver, A. Odena, C. A. Raffel, E. D. Cubuk, and I. Goodfellow. Realistic evaluation of deep semi-supervised learning algorithms. *Advances in neural information processing systems*, 31, 2018.
- A. v. d. Oord, Y. Li, and O. Vinyals. Representation learning with contrastive predictive coding. *arXiv preprint arXiv:1807.03748*, 2018.
- F. Pedregosa, G. Varoquaux, A. Gramfort, V. Michel, B. Thirion, O. Grisel, M. Blondel, P. Prettenhofer, R. Weiss, V. Dubourg, et al. Scikit-learn: Machine learning in python. *the Journal of machine Learning research*, 12:2825–2830, 2011.
- G.-J. Qi and J. Luo. Small data challenges in big data era: A survey of recent progress on unsupervised and semi-supervised methods. *IEEE Transactions on Pattern Analysis and Machine Intelligence*, 44(4):2168–2187, 2020.
- O. Russakovsky, J. Deng, H. Su, J. Krause, S. Satheesh, S. Ma, Z. Huang, A. Karpathy, A. Khosla, M. Bernstein, et al. Imagenet large scale visual recognition challenge. *International journal of computer vision*, 115:211–252, 2015.
- K. Sohn, D. Berthelot, N. Carlini, Z. Zhang, H. Zhang, C. A. Raffel, E. D. Cubuk, A. Kurakin, and C.-L. Li. Fixmatch: Simplifying semi-supervised learning with consistency and confidence. *Advances in neural information processing systems*, 33:596–608, 2020.
- E. W. Steyerberg and Y. Vergouwe. Towards better clinical prediction models: seven steps for development and an abcd for validation. *European Heart Journal*, 35(29), 2014.
- J.-C. Su, Z. Cheng, and S. Maji. A realistic evaluation of semi-supervised learning for fine-grained classification. In *Proceedings of the IEEE/CVF Conference on Computer Vision and Pattern Recognition*, pages 12966–12975, 2021.
- A. Tarvainen and H. Valpola. Mean teachers are better role models: Weight-averaged consistency targets improve semi-supervised deep learning results. *Advances in neural information processing systems*, 30, 2017.
- J. E. Van Engelen and H. H. Hoos. A survey on semi-supervised learning. *Machine learning*, 109(2): 373–440, 2020.
- A. Vaswani, N. Shazeer, N. Parmar, J. Uszkoreit, L. Jones, A. N. Gomez, Ł. Kaiser, and I. Polosukhin. Attention is all you need. *Advances in neural information processing systems*, 30, 2017.
- D. Wagner, F. Ferreira, D. Stoll, R. T. Schirrmester, S. Müller, and F. Hutter. On the importance of hyperparameters and data augmentation for self-supervised learning. *arXiv preprint arXiv:2207.07875*, 2022.
- Y. Wang, H. Chen, Y. Fan, W. Sun, R. Tao, W. Hou, R. Wang, L. Yang, Z. Zhou, L.-Z. Guo, et al. Usb: A unified semi-supervised learning benchmark for classification. *Advances in Neural Information Processing Systems*, 35:3938–3961, 2022.

- B. S. Wessler, Z. Huang, G. M. Long Jr, S. Pacifici, N. Prashar, S. Karmiy, R. A. Sandler, J. Z. Sokol, D. B. Sokol, M. M. Dehn, et al. Automated detection of aortic stenosis using machine learning. *Journal of the American Society of Echocardiography*, 36(4):411–420, 2023.
- J. Yang, R. Shi, and B. Ni. Medmnist classification decathlon: A lightweight automl benchmark for medical image analysis. In *2021 IEEE 18th International Symposium on Biomedical Imaging (ISBI)*, pages 191–195. IEEE, 2021.
- J. Yang, R. Shi, D. Wei, Z. Liu, L. Zhao, B. Ke, H. Pfister, and B. Ni. Medmnist v2-a large-scale lightweight benchmark for 2d and 3d biomedical image classification. *Scientific Data*, 10(1):41, 2023.
- S. Zagoruyko and N. Komodakis. Wide residual networks. In *Proceedings of the British Machine Vision Conference (BMVC)*, 2016.
- X. Zhai, A. Oliver, A. Kolesnikov, and L. Beyer. S4l: Self-supervised semi-supervised learning. In *Proceedings of the IEEE/CVF international conference on computer vision*, pages 1476–1485, 2019.
- B. Zhang, Y. Wang, W. Hou, H. Wu, J. Wang, M. Okumura, and T. Shinozaki. Flexmatch: Boosting semi-supervised learning with curriculum pseudo labeling. *Advances in Neural Information Processing Systems*, 34:18408–18419, 2021.
- H. Zhang, M. Cisse, Y. N. Dauphin, and D. Lopez-Paz. mixup: Beyond empirical risk minimization. *arXiv preprint arXiv:1710.09412*, 2017.
- M. Zheng, S. You, L. Huang, F. Wang, C. Qian, and C. Xu. Simmatch: Semi-supervised learning with similarity matching. In *Proceedings of the IEEE/CVF Conference on Computer Vision and Pattern Recognition*, pages 14471–14481, 2022.
- X. Zhu, Z. Ghahramani, and J. D. Lafferty. Semi-supervised learning using gaussian fields and harmonic functions. In *Proceedings of the 20th International conference on Machine learning (ICML-03)*, pages 912–919, 2003.
- X. J. Zhu. Semi-supervised learning literature survey. 2005.
- F. Zhuang, Z. Qi, K. Duan, D. Xi, Y. Zhu, H. Zhu, H. Xiong, and Q. He. A comprehensive survey on transfer learning. *Proceedings of the IEEE*, 109(1):43–76, 2020.

Appendix Contents

A	Additional Results	15
A.1	Impact of pretraining on accuracy-over-time profiles	15
A.2	Comparing validation vs. test profiles of accuracy-over-time	16
A.3	Histograms of accuracy	17
A.4	Balanced Accuracy over time across trials	17
B	Algorithms Details	18
B.1	Algorithm : Random Hyperparameter search on a budget	18
B.2	Hyperparameter transfer strategy	19
B.3	Semi-supervised method details.	19
B.4	Self-supervised method details	19
C	Hyperparameter Details	21
C.1	Search Range	21
C.2	Chosen Hyperparameters on TissueMNIST	23

A Additional Results

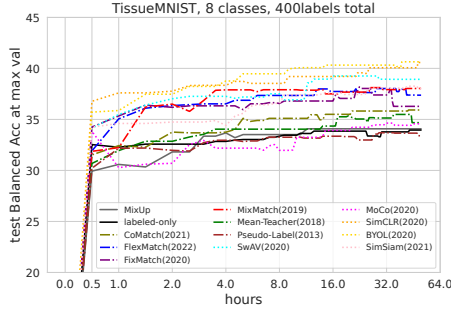
A.1 Impact of pretraining on accuracy-over-time profiles

Fig. A.1 shows how the accuracy-over-time profiles on the two lightweight datasets (Tissue and Path) vary based on the initialization strategy: left column uses a pretraining on ImageNet strategy, right column uses a random initial weights strategy.

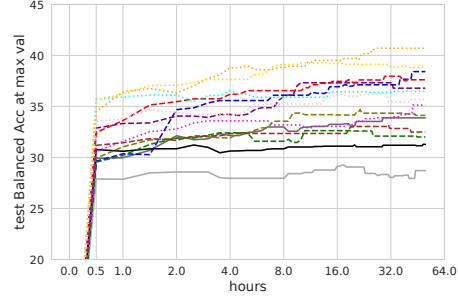
On TissueMNIST, SimCLR (yellow) and BYOL (orange) are the top two methods in both cases.

On PathMNIST, semi-supervised methods dominate: FixMatch and CoMatch are best on the pretraining case, with MixMatch and Flexmatch only a few points of balanced accuracy lower. MixMatch and CoMatch are best in the random case.

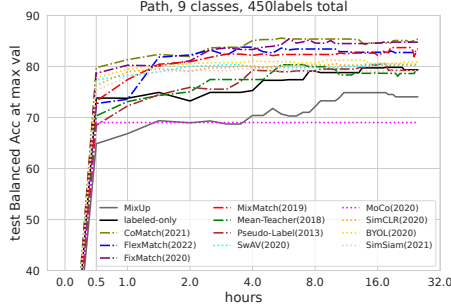
Across both plots, pretraining does not seem to impact the top-performing methods ultimate accuracy too much (e.g. by more than a few points of accuracy). However, with more limited time budgets (e.g. after only a few hours), we do see initialization from pretraining understandably tends to improve some methods. Pretraining time on a source dataset is NOT counted to the runtime reported in x-axis.



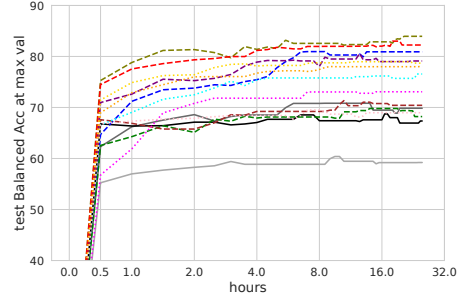
(a) TissueMNIST : pretrained initial weights



(b) TissueMNIST : random initial weights



(c) PathMNIST : pretrained initial weights



(d) PathMNIST: random initial weights

Figure A.1: **Balanced accuracy on test set over time for semi- and self-supervised methods, with (left) and without (right) initial weight pretraining on ImageNet.** Curves represent mean of each method at each time over 5 trials of Alg. 1. On TissueMNIST (a), SimCLR (orange) and BYOL (yellow) are dominant from 1 hour onward. On PathMNIST (b), MixMatch (red) is dominant from 1 hour onward, unsurpassed by the more recent FixMatch and FlexMatch. On TMED-2 (c), Sup Contrast wins for first 7 hours, then MixMatch overtakes it, eventually joined (but not surpassed) by FixMatch and FlexMatch.

A.2 Comparing validation vs. test profiles of accuracy-over-time

Fig. A.2 shows profiles of accuracy over time on the validation set, in contrast to the test set performance shown in the main paper’s Fig. 1.

All curves here by definition must be monotonically increasing, because our unified algorithm selects new checkpoints only when they improve the validation-set balanced accuracy metric. The important insight our work reveals is that the same model checkpoints selected here, based on validation-set accuracy, also tend to produce improved test-set accuracy over time (in Fig. 1). This helps provide empirical confidence in using realistically-sized validation sets.

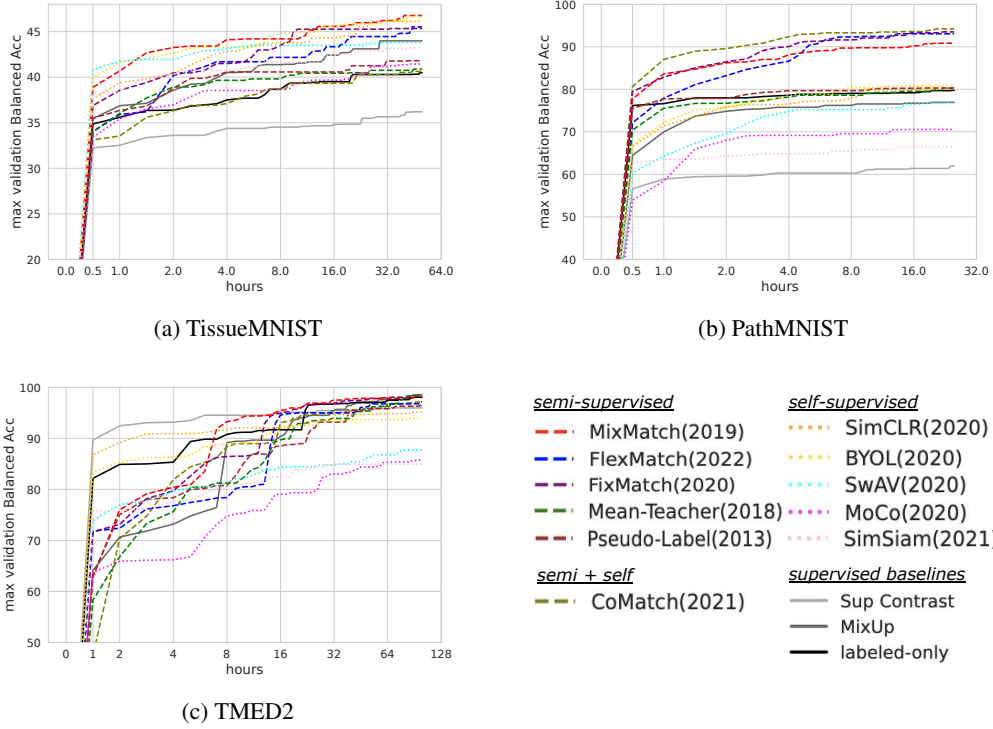


Figure A.2: **VALIDATION** accuracy over time profiles of semi- and self-supervised methods on 3 datasets (panels a-c). In contrast to the test plot, the semi-supervised methods prove to be dominant across all three datasets. For TissueMNIST and TMED2, the performance ranking on the validation set aligns consistently with that on the test accuracy. Despite semi-supervised methods demonstrating superior performance on the PathMNIST validation set, self-supervised methods outperform on the corresponding test set.

A.3 Histograms of accuracy

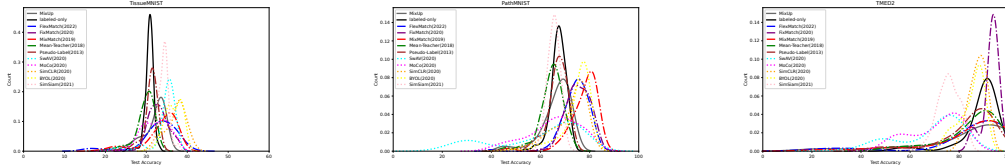


Figure A.3: Distribution of test accuracy that corresponded to the maximum validation accuracy. From left to right are TissueMNIST, PathMNIST and TMED2.

A.4 Balanced Accuracy over time across trials

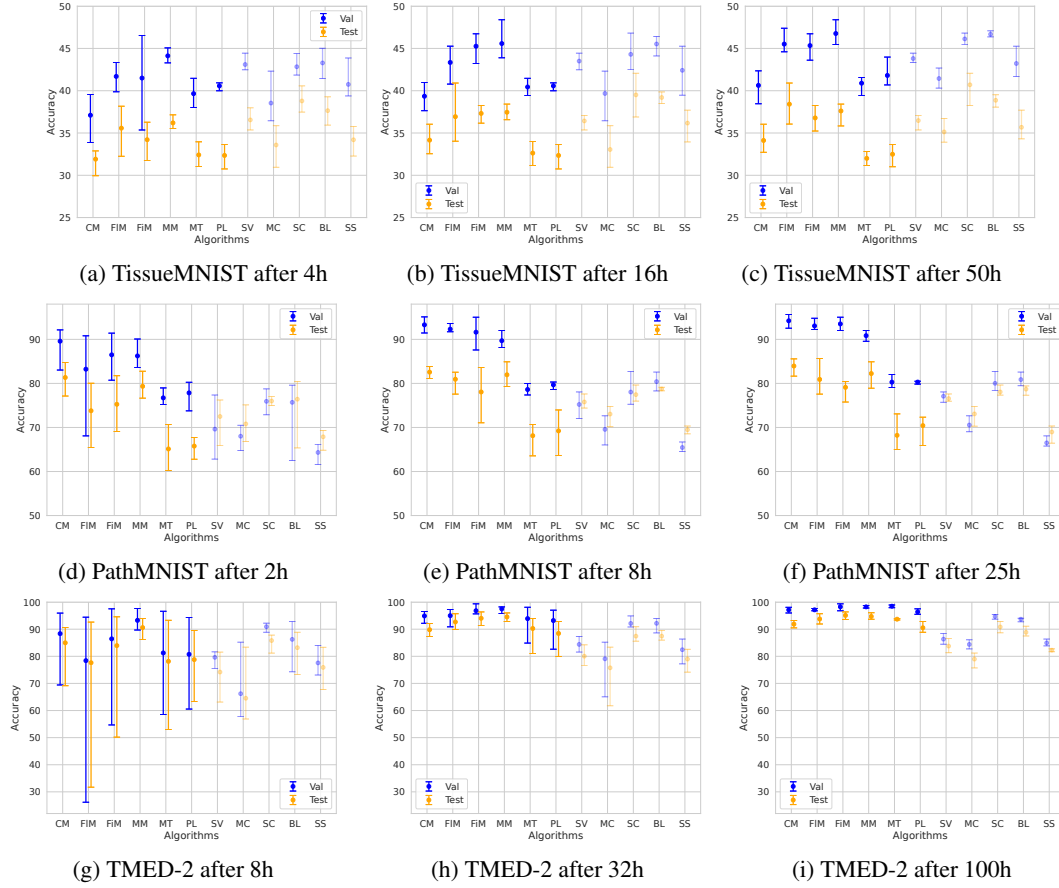


Figure A.4: Balanced accuracy for different methods across 3 time budgets (columns) and three datasets (rows). For each method, the intervals indicate the low and high performance of 5 separate trials of Alg. B.1. Dots indicate mean performance across all 5 trials.

B Algorithms Details

B.1 Algorithm : Random Hyperparameter search on a budget

Algorithm B.1 outlines our uniform hyperparameter tuning procedures used across all algorithms under comparison. The algorithm requires three sources of data: a labeled training set $\mathcal{L} = \{X, Y\}$, an unlabeled set for training $\mathcal{U} = X^U$, and a separate realistically-sized labeled validation set $\{X^{val}, Y^{val}\}$. We further require some budget restrictions: a common computational budget T (maximum number of hours), and a maximum training epoch per hyperparameter configuration E .

We proceed as follows: We begin by randomly sampling a hyperparameter configuration from a defined range (see Appendix C.1 for details). A model is then initialized and trained using the ADAM optimizer with the sampled hyperparameters. Each configuration is trained for a maximum of E (200) epochs or stopped early if the validation performance does not improve for 20 consecutive epochs. The model’s performance on the validation set is measured using balanced accuracy. Upon completion of training for a given hyperparameter configuration (either after reaching maximum epoch E or after early stopping), a new configuration is sampled and the process repeats until the total compute budget T is expended.

We track the best-so-far model performance every 30 minutes, and save the best-so-far model and its corresponding validation and test performance. Semi-supervised algorithms simultaneously train the representation layers v and classifier layer w , while self-supervised algorithms train the representation layers v for each epoch and then fine-tune a linear classifier with weights w anew at the end of each epoch using sklearn logistic regression model (Pedregosa et al., 2011) with representation parameters v frozen.

Algorithm B.1 Unified Procedure for Training + Hyperparameter selection via random search

Input: • Train set of features \mathbf{X} paired with labels \mathbf{Y} , with extra unlabeled features \mathbf{U}

- Validation set of features \mathbf{X}^{val} and labels \mathbf{Y}^{val}
- Runtime budget T , Max Epoch E

Output: Trained weights $\{v, w\}$, where v is representation module, w is classifier layer

Procedure

```

1: while time elapsed <  $T$  do
2:    $\lambda \sim \text{DRAWHYPER}$  ▷ Sample hyperparameters for random search
3:    $\xi \leftarrow \text{CREATEOPTIM}(\lambda)$  ▷ Initialize stateful optimizer e.g. ADAM
4:    $\{v, w\} \sim \text{INITWEIGHTS}$  ▷ Initialize model weights
5:   for epoch  $e$  in  $1, 2, \dots E$  do
6:     if self-supervised then
7:        $v \leftarrow \text{TRAINONEEPOCH}(\mathbf{U}, v, \lambda, \xi)$  ▷ Optimize Eq. (1) with  $\lambda^L = 0$ 
8:        $w \leftarrow \text{TRAINCLASSIFIER}(\mathbf{Y}, f_v(\mathbf{X}))$ 
9:     else if semi-supervised then
10:       $v, w \leftarrow \text{TRAINONEEPOCH}(\mathbf{X}, \mathbf{Y}, \mathbf{U}, v, w, \lambda, \xi)$  ▷ Optimize Eq. (1)
11:     else
12:       $v, w \leftarrow \text{TRAINONEEPOCH}(\mathbf{X}, \mathbf{Y}, v, w, \lambda, \xi)$  ▷ Optimize Eq. (1) with  $\lambda^U = 0$ 
13:     end if
14:      $m_e \leftarrow \text{CALCBALACC}(\mathbf{X}^{val}, \mathbf{Y}^{val}, v, w)$  ▷ Record performance metric on val.
15:     if first try or  $m_e > m_*$  then ▷ Update best config found so far
16:        $v_*, w_* \leftarrow v, w; \lambda_* \leftarrow \lambda; m_* \leftarrow m_e$ 
17:     end if
18:     if  $\text{EARLYSTOP}(m_1, m_2, \dots m_e)$  or time elapsed >  $T$  then
19:       break
20:     end if
21:   end for
22: end while
23: return  $v_*, w_*, \lambda_*, m_*$ 

```

B.2 Hyperparameter transfer strategy

To make the most of limited labeled data, one potential strategy is to use the entire labeled set for training, reserving no validation set at all, and thus relies on pre-established hyperparameters from other dataset/experiments. In this study, we experiment with two scenarios: using pre-determined hyperparameters from 1. CIFAR-10, or 2. TissueMNIST. The CIFAR-10 hyperparameters are sourced from public repositories, we ensure that our CIFAR-10 hyperparameter choices on our re-implementation of the algorithms matches previously reported results in the literature. The TissueMNIST hyperparameters originate from our experiments as depicted in Figure A.2 (a).

B.3 Semi-supervised method details.

Semi-supervised learning trains on the labeled and unlabeled data simultaneously, usually with the total loss being a weighted sum of a labeled loss term and an unlabeled loss term. Different methods mainly differs in how unlabeled data is used to form training signals. Many approaches have been proposed and refined over the past decades. These include co-training, which involves training multiple classifiers on various views of the input data (Blum and Mitchell, 1998; Min et al., 2020); graph-structure-based models (Zhu et al., 2003; Iscen et al., 2019); generative models (Kingma et al., 2014; Kumar et al., 2017); consistency regularization-based models that enforce consistent model outputs (Laine and Aila, 2016; Tarvainen and Valpola, 2017; Berthelot et al., 2019); pseudo label-based models that impute labels for unlabeled data (Lee, 2013; Cascante-Bonilla et al., 2021); and hybrid models that combines several methods (Sohn et al., 2020). Comprehensive reviews can be found in Zhu (2005); Chapelle et al. (2009); Van Engelen and Hoos (2020).

Among the deep classifier methods following Eq. (1), below we describe each method we selected and how its specific unlabeled loss is constructed.

Pseudo-Labeling uses the current model to assign class probabilities to each sample in the unlabeled batch. If, for an unlabeled sample, the maximum class probability $P(y_i)$ exceeds a certain threshold τ , this sample contributes to the calculation of the unlabeled loss for the current batch. The cross-entropy loss is computed as if the true label of this sample is class i .

Mean-Teacher constructs the unlabeled loss by enforcing consistency between the model’s output for a given sample and the output of the same sample from the Exponential Moving Average (EMA) model.

MixMatch uses the MixUp (Zhang et al., 2017) technique on both labeled data (features and labels) and unlabeled data (features and guessed labels) within each batch to produce transformed labeled and unlabeled data. The labeled and unlabeled losses are then calculated using these transformed samples. Specifically, the unlabeled loss is derived from the mean squared error between the model’s output for the transformed unlabeled samples and their corresponding transformed guessed labels.

FixMatch generates two augmentation of an unlabeled sample, one with weak augmentation and the other using strong augmentations (e.g., RandAug (Cubuk et al., 2020)). The unlabeled loss is then formulated by enforcing the model’s output for the strongly augmented sample to closely resemble that of the weakly augmented sample using cross-entropy loss.

FlexMatch builds directly upon FixMatch by incorporating a class-specific threshold on the unlabeled samples during training.

CoMatch marks the first introduction of contrastive learning into semi-supervised learning. The model is equipped with two distinct heads: a classification head, which outputs class probabilities for a given sample, and a projection head, which maps the sample into a low-dimensional embedding. These two components interact in a unique manner. The projection head-derived embeddings inform the similarities between different samples, which are then used to refine the pseudo-labels against which the classification head is trained. Subsequently, these pseudo-labels constitute a pseudo-label graph that trains the embedding graph produced by the projection head.

B.4 Self-supervised method details

In recent years, self-supervised learning algorithms have emerged rapidly and are known as one of the most popular field of machine learning. These include contrastive learning, which involves

learning representations by maximizing agreement between differently augmented views of the same data (Chen et al., 2020b; He et al., 2020); predictive models that forecast future instances in the data sequence (Oord et al., 2018); generative models that learn to generate new data similar to the input (Chen et al., 2020a); clustering-based approaches that learn representations by grouping similar instances (Caron et al., 2018, 2020); context-based models that predict a specific part of the data from other parts (Devlin et al., 2018; Brown et al., 2020); and hybrid models that combine various methods for more robust learning (Chen et al., 2020c). A more comprehensive review can be found in (Jing and Tian, 2020; Zhuang et al., 2020).

Below, we provide for each selected self-supervised method a summary of its internal workings.

SimCLR generates two augmented versions of each image. Then feed these pairs of images into a base encoder network to generate image embeddings. This encoder is followed by a projection head, which is a multilayer neural network, to map these embeddings to a space where contrastive loss can be applied. Next, calculate the contrastive loss. The idea is to make the embeddings of augmented versions of the same image (positive pairs) as similar as possible and to push apart embeddings from different images (negative pairs). The loss function used is NCE loss.

MOCO V2 creates two augmented versions of each image. These pairs are processed by two encoder networks: a query encoder, and a key encoder updated by a moving average of the query encoder. The contrastive loss is computed by comparing a positive pair (the query and corresponding key) against numerous negative pairs drawn from a large queue of keys.

Note on runtime: We notice that the performance on MoCo can be increased when Shuffling BN across multiple GPUs. However, to ensure a fair comparison given our single-GPU setup, we refrained from employing any techniques to simulate multiple GPUs on one, as this would change the encoder’s structure.

SwAV begins by creating multiple augmented versions of each image. Then, these versions are input into a deep neural network to generate embeddings. Uses a clustering approach, called online stratified sampling, to predict assignments of each view’s prototypes (or cluster centers) to others, encouraging the model to match the representations of different augmentations of the same image.

Note on runtime: We’ve observed that applying multiple augmentations can enhance the effectiveness of various methods. To prevent the results from being influenced by these augmentations, we’ve standardized the number of augmentations to two in SwAV, in line with the approach taken by other methods.

BYOL starts by creating two differently augmented versions of each image. These versions are processed through two identical neural networks, known as the target and online networks, which include a backbone and a projection head. The online network is updated through backpropagation, while the target network’s weights are updated as a moving average of the online network’s weights. The unique aspect of BYOL is that it learns representations without the need for negative samples.

SimSiam creates two differently augmented versions of each image. These versions are passed through two identical networks: one predictor network and one encoder network. The encoder network contains a backbone and a projection head.

C Hyperparameter Details

Below we show the search range of each hyperparameter.

C.1 Search Range

Shared By All	
Optimizer	Adam
Learning rate schedule	Cosine
Labeled only	
Batch size	64
Learning rate	$3 \times 10^x, X \sim \text{Uniform}(-5, -2)$
Weight decay	$4 \times 10^x, X \sim \text{Uniform}(-6, -3)$
MixUp	
Batch size	64
Learning rate	$3 \times 10^x, X \sim \text{Uniform}(-5, -2)$
Weight decay	$4 \times 10^x, X \sim \text{Uniform}(-6, -3)$
Beta shape α	$x, X \sim \text{Uniform}(0.1, 10)$
Sup Contrast	
Batch size	256
Learning rate	$3 \times 10^x, X \sim \text{Uniform}(-5.5, -1.5)$
Weight decay	$4 \times 10^x, X \sim \text{Uniform}(-7.5, -3.5)$
Temperature	$x, X \sim \text{Uniform}(0.05, 0.15)$
FlexMatch	
Labeled batch size	64
Unlabeled batch size	448
Learning rate	$3 \times 10^x, X \sim \text{Uniform}(-5, -2)$
Weight decay	$4 \times 10^x, X \sim \text{Uniform}(-6, -3)$
Unlabeled loss coefficient	$10^x, X \sim \text{Uniform}(-1, 1)$
Unlabeled loss warmup schedule	No warmup
Pseudo-label threshold	0.95
Sharpening temperature	1.0
FixMatch	
Labeled batch size	64
Unlabeled batch size	448
Learning rate	$3 \times 10^x, X \sim \text{Uniform}(-5, -2)$
Weight decay	$4 \times 10^x, X \sim \text{Uniform}(-6, -3)$
Unlabeled loss coefficient	$10^x, X \sim \text{Uniform}(-1, 1)$
Unlabeled loss warmup schedule	No warmup
Pseudo-label threshold	0.95
Sharpening temperature	1.0
CoMatch	
Labeled batch size	64
Unlabeled batch size	448
Learning rate	$3 \times 10^x, X \sim \text{Uniform}(-5, -2)$
Weight decay	$4 \times 10^x, X \sim \text{Uniform}(-6, -3)$
Unlabeled loss coefficient	$10^x, X \sim \text{Uniform}(-1, 1)$
Unlabeled loss warmup schedule	No warmup
Contrastive loss coefficient	$5 \times 10^x, X \sim \text{Uniform}(-1, 1)$
Pseudo-label threshold	0.95
Sharpening temperature	0.2

For TMED2, unlabeled batch size is set to 320 to reduce GPU memory usage

MixMatch		
Labeled batch size		64
Unlabeled batch size		64
Learning rate	$3 \times 10^x, X \sim \text{Uniform}(-5, -2)$	
Weight decay	$4 \times 10^x, X \sim \text{Uniform}(-6, -3)$	
Beta shape α	$x, X \sim \text{Uniform}(0.1, 1)$	
Unlabeled loss coefficient	$7.5 \times 10^x, X \sim \text{Uniform}(0, 2)$	
Unlabeled loss warmup schedule		linear
Sharpening temperature		0.5

Mean Teacher		
Labeled batch size		64
Unlabeled batch size		64
Learning rate	$3 \times 10^x, X \sim \text{Uniform}(-5, -2)$	
Weight decay	$4 \times 10^x, X \sim \text{Uniform}(-6, -3)$	
Unlabeled loss coefficient	$8 \times 10^x, X \sim \text{Uniform}(-1, 1)$	
Unlabeled loss warmup schedule		linear

Pseudo-label		
Labeled batch size		64
Unlabeled batch size		64
Learning rate	$3 \times 10^x, X \sim \text{Uniform}(-5, -2)$	
Weight decay	$4 \times 10^x, X \sim \text{Uniform}(-6, -3)$	
Unlabeled loss coefficient	$10^x, X \sim \text{Uniform}(-1, 1)$	
Unlabeled loss warmup schedule		Linear
Pseudo-label threshold		0.95

SwAV		
Batch size		256
Learning rate	$1 \times 10^x, X \sim \text{Uniform}(-4.5, -1.5)$	
Weight decay	$1 \times 10^x, X \sim \text{Uniform}(-6.5, -3.5)$	
Temperature	$x, X \sim \text{Uniform}(0.07, 0.12)$	
number of prototypes	$1 \times 10^x, X \sim \text{Uniform}(1, 3)$	

MoCo		
Batch size		256
Learning rate	$1 \times 10^x, X \sim \text{Uniform}(-4.5, -1.5)$	
Weight decay	$1 \times 10^x, X \sim \text{Uniform}(-6.5, -3.5)$	
Temperature	$x, X \sim \text{Uniform}(0.07, 0.12)$	
Momentum	$x, X \sim \text{Uniform}(0.99, 0.9999)$	

SimCLR		
Batch size		256
Learning rate	$1 \times 10^x, X \sim \text{Uniform}(-4.5, -1.5)$	
Weight decay	$1 \times 10^x, X \sim \text{Uniform}(-6.5, -3.5)$	
Temperature	$x, X \sim \text{Uniform}(0.07, 0.12)$	

SimSiam		
Batch size		256
Learning rate	$1 \times 10^x, X \sim \text{Uniform}(-4.5, -1.5)$	
Weight decay	$1 \times 10^x, X \sim \text{Uniform}(-6.5, -3.5)$	

BYOL		
Batch size		256
Learning rate	$1 \times 10^x, X \sim \text{Uniform}(-4.5, -1.5)$	
Weight decay	$1 \times 10^x, X \sim \text{Uniform}(-6.5, -3.5)$	
Temperature	$x, X \sim \text{Uniform}(0.07, 0.12)$	
Momentum	$x, X \sim \text{Uniform}(0.99, 0.9999)$	

In practice, we round each sampled α value to the nearest tenth decimal place

C.2 Chosen Hyperparameters on TissueMNIST

Below we report the chosen hyperparameters on TissueMNIST that are used in the hyperparameter transfer experiments.

FlexMatch					
	seed0	seed1	seed2	seed3	seed4
Learning rate	0.00036	0.00016	0.00016	0.00068	0.00006
Weight decay	0.00259	0.00001	0.00371	0.00023	0.002103
Unlabeled loss coefficient	2.22	0.82	5.00	1.94	6.09
FixMatch					
	seed0	seed1	seed2	seed3	seed4
Learning rate	0.00074	0.00034	0.00392	0.00102	0.00037
Weight decay	0.00045	0.00315	0.00001	0.00005	0.00058
Unlabeled loss coefficient	3.08	6.70	1.85	1.46	0.47
CoMatch					
	seed0	seed1	seed2	seed3	seed4
Learning rate	0.00124	0.00145	0.00061	0.00026	0.00113
Weight decay	0.00042	0.00009	0.00005	0.00009	0.00017
Unlabeled loss coefficient	0.30	1.71	1.26	2.74	0.46
Contrastive loss coefficient	1.26	2.21	3.71	0.56	1.37
MixMatch					
	seed0	seed1	seed2	seed3	seed4
Learning rate	0.00028	0.00003	0.00018	0.00009	0.00005
Weight decay	0.000005	0.00195	0.00005	0.00085	0.00082
Beta shape α	0.2	0.9	0.9	0.8	0.7
Unlabeled loss coefficient	9.13	37.96	8.06	25.16	11.17
Mean Teacher					
	seed0	seed1	seed2	seed3	seed4
Learning rate	0.00062	0.00022	0.00005	0.00128	0.00125
Weight decay	0.00189	0.00001	0.00008	0.00001	0.00001
Unlabeled loss coefficient	67.67	0.87	1.25	7.60	13.56
Pseudo-label					
	seed0	seed1	seed2	seed3	seed4
Learning rate	0.00007	0.00021	0.00005	0.00063	0.00060
Weight decay	0.00033	0.00093	0.00383	0.00005	0.00087
Unlabeled loss coefficient	0.19	0.16	8.73	0.82	0.25
SwAV					
	seed0	seed1	seed2	seed3	seed4
Learning rate	0.00065	0.00325	0.00012	0.00086	0.00196
Weight decay	0.0001497	0.0000056	0.0000006	0.0000021	0.0000003
Number of prototypes	845	131	36	201	59
MoCo					
	seed0	seed1	seed2	seed3	seed4
Learning rate	0.00288	0.00023	0.00043	0.00005	0.02629
Weight decay	0.000002	0.0000008	0.0000003	0.0000005	0.0000004
temperature	0.09331	0.07097	0.10987	0.07414	0.07080
Momentum	0.99242	0.99672	0.99267	0.99950	0.99538
SimCLR					
	seed0	seed1	seed2	seed3	seed4
Learning rate	0.00217	0.00131	0.000640	0.00380	0.00136
Weight decay	0.00002	0.00001	0.00001	0.00001	0.00001
temperature	0.11719	0.10426	0.08652	0.07784	0.11478

SimSiam					
	seed0	seed1	seed2	seed3	seed4
Learning rate	0.0002	0.00056	0.00013	0.00338	0.00098
Weight decay	0.000066	0.000046	0.000023	0.000001	0.000001
BYOL					
	seed0	seed1	seed2	seed3	seed4
Learning rate	0.000245	0.001308	0.000371	0.001653	0.001959
Weight decay	0.0000007	0.0000057	0.0000004	0.000003	0.000001
Momentum	0.9928618	0.996167	0.9988484	0.9940063	0.9934791